

Spin-density-wave clusters in $\text{Pd}_{1-x}\text{Cr}_x$ spin-glass alloys

Masaya Hirano and Yorihiro Tsunoda

Department of Applied Physics, School of Science and Engineering, Waseda University, 3-4-1 Okubo, Shinjuku, Tokyo, 169-8555, Japan
(Received 10 November 1998)

Susceptibility and neutron scattering measurements were performed for $\text{Pd}_{1-x}\text{Cr}_x$ ($x=0.075, 0.11, 0.15$) alloy single crystals. In neutron scattering measurements, satellite diffuse peaks were observed at $1 \pm \delta$ 0 0 positions at low temperature. The satellite peak position varies with Cr concentration, but the peak linewidth is not sensitive to the solute concentration. Satellite peaks disappear far above the freezing temperature at which the cusp-type anomaly is observed in susceptibility measurement. Origin of the spin-glass-like behavior of PdCr alloys is ascribed to the fluctuating spin-density-wave clusters as is observed for the typical spin-glass alloys CuMn. [S0163-1829(99)07421-4]

I. INTRODUCTION

The mysterious magnetic behavior in CuMn alloys, which have long been looked upon as a typical spin glass is recently explained by the formation of spin density wave (SDW) clusters: in neutron scattering experiments satellite reflections with a rather wide linewidth are observed at $1 \frac{1}{2} \pm \eta$ 0.^{1,2} Strong inelastic scattering is also observed at the satellite peak positions even at far higher temperature than the freezing temperature T_F .³ Thus, the dynamical motion and freezing process of the SDW clusters would play essential roles in the spin-glass-like behavior of this system. Since the SDW satellite peak position varies with Mn concentration the origin of the SDW formation is considered to be a reflection of the parallel planes of Fermi surfaces in CuMn alloys.⁴ This result for CuMn alloys stimulated the studies of other metallic spin-glass alloys. A recent neutron scattering experiment revealed that the same mechanism brought about the spin-glass-like behavior for PdMn alloys, although the wave vector of the SDW is completely different from that in CuMn alloys because of the difference of the shape of Fermi surfaces in host metals.⁵

PdCr alloys containing more than 7 at. % Cr show the spin-glass-like behavior.⁶ Unlike other alloys, since the ordered phase Pd_3Cr is not discovered for this alloy, the spin-glass-like behavior can be observed up to relatively high Cr concentration. The previous authors studied the susceptibility of $\text{Pd}_{75}\text{Cr}_{25}$ disordered alloy and pointed out that the origin of the spin-glass-like behavior for $\text{Pd}_{75}\text{Cr}_{25}$ would be the same as the disordered Pd_3Mn alloy.⁷

In the present paper, by means of the neutron scattering experiments and the susceptibility data, we report that the spin-glass-like behavior in PdCr alloys is again ascribed to the formation of the SDW clusters. PdCr alloys differ from PdMn alloys in a solute and from CuMn alloys in both solvent and solute. Thus, we claim here that the fluctuating SDW clusters are fundamental mechanisms for the alloys to show spin-glass-like behavior and common for several metallic spin-glass alloys such as CuMn, AgMn, PdMn, PtMn, and PdCr.

On the other hand, in the region with less than 7 at. % Cr these alloys are considered to be nonmagnetic.⁶ The mag-

netic moments of Cr atoms are screened out by the conduction electrons (Kondo singlet state) because of high Kondo temperature ($T_1 \approx 100$ K).⁸ We also discuss this problem briefly.

II. SAMPLE PREPARATION AND EXPERIMENTS

Three single crystal specimens of PdCr alloys with Cr concentration 7.5, 11, and 15 at. % were prepared for the present experiments. Pd with a purity of 99.95% and Cr with 99.999% were used as raw materials for these single crystals, which were grown by the Bridgman method in the furnace with a carbon heater system under an Ar gas atmosphere and then cooled down in the furnace. Since the temperature inside the furnace fell down at a speed of about 200 °C a minute the cooling speed is rather high, though not so quick as that of quenching. Single crystals have a volume of about 1 cc and were used for neutron scattering and susceptibility measurements in the as-grown state.

The susceptibility was measured using a superconducting quantum interference device (SQUID) system at the Materials Characterization Central Laboratory, Waseda University, in a magnetic field of 200 G. For the susceptibility measurements small pieces of about 0.01 cc were cut off from each single crystal ingot and the rest was used for the neutron scattering measurements.

The neutron scattering measurements for the specimens of 11 and 15 at. % Cr alloys were performed at the T1-1 triple axis spectrometer installed at a thermal guide, JRR-3M. Tokai and the data for 7.5 at. % Cr alloy were taken at the 5 G (PONTA) triple axis spectrometer installed at a reactor room of JRR-3M to obtain the high flux beam. Incident neutrons with energy of 14 meV were used for all measurements. A refrigerator unit was used for lowering the temperature of the specimens.

III. EXPERIMENTAL DATA

Susceptibility measurements

The temperature-dependent susceptibility data for the present specimens are summarized in Fig. 1. The data were

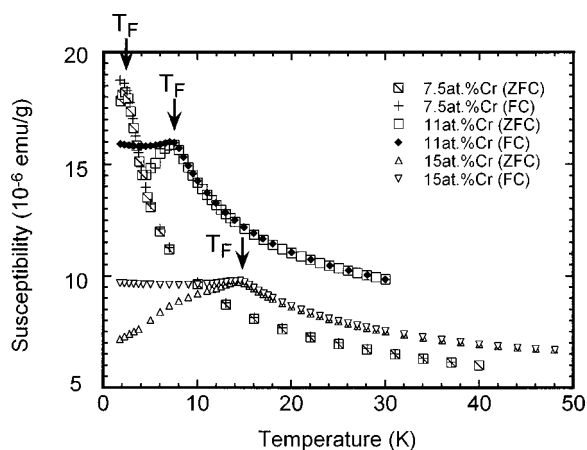


FIG. 1. Susceptibility data for PdCr alloys. ZFC and FC indicate that samples were cooled in zero field and in the field of 200 G, respectively.

obtained as follows. At first the specimens were cooled down to 1.7 K in zero field, then the susceptibility was measured in the field of 200 G with raising temperature. This warming curve shows a cusp-type peak at the freezing temperature T_F . After reaching the highest temperature, the specimen was cooled down keeping the field at 200 G. This cooling curve traces the same path as the warming one above T_F . Below T_F , however, it shows remanence. This is a typical behavior of the spin-glass alloys. All of our specimens show the typical spin-glass behavior and are consistent with previous PdCr data.⁶ The Cr concentration variations of T_F are given in Fig. 2, together with the data reported by the previous authors for comparison. Freezing temperature is described as a linear function of Cr concentration and the extrapolation to 0 K crosses at around 7 at. % Cr.

Neutron scattering measurements

Neutron diffraction patterns observed at 7 and 300 K for 15 at. % Cr alloy are given in Fig. 3. These data were taken by scanning along the [100] axis passing through the 100 reciprocal lattice point. Figure 3 shows that the diffraction pattern observed at 7 K has diffuse satellite peaks at $1 \pm \delta$ 0

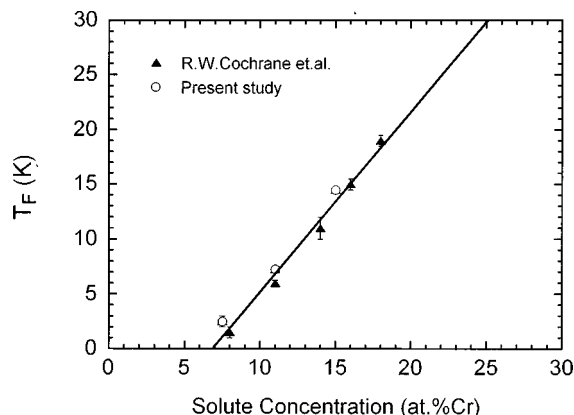


FIG. 2. Cr-concentration variation of the freezing temperature. The data from previous authors are also shown by solid triangles.

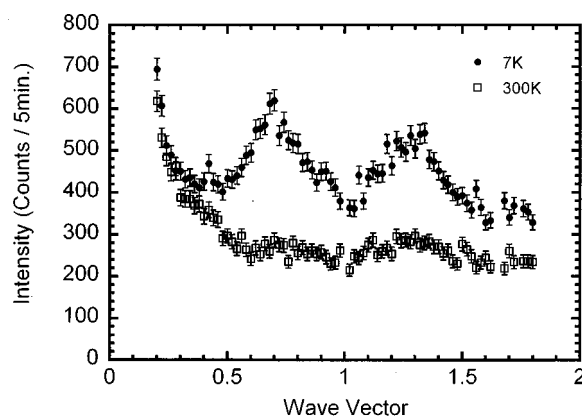


FIG. 3. Neutron diffraction patterns for Pd₈₅Cr₁₅ observed by scanning along the [100] axis at 7 and 300 K.

0 ($\delta=0.282$) position but they disappear at 300 K. The intensities of these satellite peaks therefore are temperature-dependent. The temperature-dependent diffraction component obtained by subtracting the 300 K data from the 7 K data is given in Fig. 4(a). The diffraction patterns obtained by the same way for 11 and 7.5 at. % Cr alloys are given in Figs. 4(b) and 4(c), respectively. An asymmetric intensity for both sides of satellite peaks for all data is probably due to the wave vector dependence of the magnetic form factor and this supports that the temperature-dependent satellite peaks are magnetic in origin. Since the data for 7.5 at. % Cr alloy were taken at the high flux machine, 5 G triple axis spectrometer absolute intensity is not comparable with other data. The

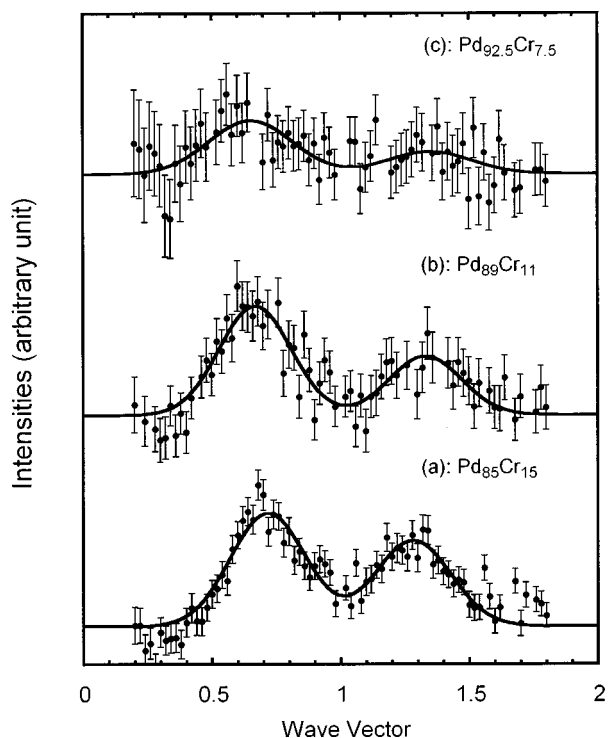


FIG. 4. Temperature dependent satellite component for (a) 15 at. % Cr, (b) 11 at. % Cr, and (c) 7.5 at. % Cr. The value of intensity for each sample is arbitrary. Solid lines indicate the best fitting curves (see text).

TABLE I. Satellite peak positions and correlation lengths for $\text{Pd}_{1-x}\text{Cr}_x$ alloys determined by the least square fitting using double Gaussian line profiles.

Sample	Peak position δ	Linewidth (a^* unit)	Correlation length ($/a^*$)
$\text{Pd}_{92.5}\text{Cr}_{7.5}$	0.349	0.37	2.70
$\text{Pd}_{89}\text{Cr}_{11}$	0.315	0.36	2.78
$\text{Pd}_{85}\text{Cr}_{15}$	0.282	0.40	2.50

satellite peaks were also studied along the direction perpendicular to the $[100]$ axis. The diffuse peak linewidth is comparable with that for the longitudinal scan. Thus, the short-range spin correlation develops roughly spherically.

In Figs. 4(a)–4(c), solid lines are least-square fits using a constant background plus double Gaussian peaks with parameters representing peak height, peak position and linewidth. Peak position and linewidth of each specimen are summarized in Table I. The line broadening due to the instrumental resolution is negligibly small compared with the diffuse peak line width observed here. Magnetic correlation length in PdCr alloys is estimated from the linewidth to be about 2.5 times the lattice parameter and not sensitive to the Cr concentration. On the other hand, peak position sensitively depends on the Cr concentration.

The temperature variations of the satellite peak intensities at $1 - \delta \ 0 \ 0$ position for 11 at. % Cr and 15 at. % Cr alloys are given in Fig. 5. In this figure, the intensity is normalized to the value at the lowest temperature for each specimen and the arrows indicate the freezing temperature (T_F) obtained by the susceptibility measurements. The satellite peaks disappear at the temperatures far above T_F and the satellite peak intensity continuously changes at T_F . These features are common to the spin-glass alloys with the SDW clusters, such as CuMn (Ref. 1) and PdMn.⁵ This is due to the broadness of the time resolution window in neutron scattering experiment. Although we used analyzer crystal to eliminate inelastic scattering, dynamical process moving slower than 10^{11}Hz is still observed as elastic scattering in the present measurements.

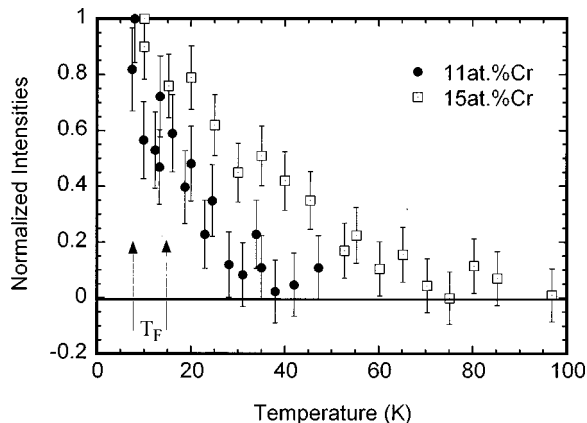


FIG. 5. Temperature dependence of the normalized intensities studied at $1 - \delta \ 0 \ 0$ satellite peak position for $\text{Pd}_{89}\text{Cr}_{11}$ and $\text{Pd}_{85}\text{Cr}_{15}$.

IV. DISCUSSIONS

Previously, susceptibility and resistivity data were reported for PdCr alloys with relevant Cr concentration region by Cochrane *et al.*,⁶ Roshko *et al.*,⁹ and Kao *et al.*,¹⁰ respectively. As we mentioned in the preceding section, our susceptibility data are consistent with their data. However, there are no neutron scattering experiments comparable with the present investigation. Thus, we will try to compare the present data with those on another alloy, PdMn, which exhibits similar spin-glass-like susceptibility. The PdMn alloy shows a mysterious magnetic phase diagram. The alloys containing less than 2.5 at. % Mn are in a ferromagnetic phase, which is recognized as exchange enhanced ferromagnet, while the alloys with more than 5 at. % Mn are in the spin-glass phase. The alloys from 2.5 to 5 at. % Mn are in mixed ordering.¹¹ Whereas the magnetic phase diagram of PdCr (Fig. 2) is very simple. The alloys with Cr concentration more than about 7 at. % are in spin-glass phase, but those with less than about 7 at. % Cr are nonmagnetic. Note that both PdCr and PdMn alloys in the spin-glass phase exhibit similar behavior in the susceptibility. As the solute concentration decreases absolute value of the susceptibility increases. Since PdMn alloys with low Mn concentration show ferromagnetic long range order, this behavior might be consistent with the phase diagram. However, increasing of the susceptibility for low Cr concentration must be ascribed to different origin. One of the possible explanation stands on a short-range SDW. As the Cr concentration decreases the wavelength of the SDW elongates but the correlation length remains unchanged. If the wavelength is larger than the correlation length, the SDW is incomplete and ferromagnetic component remains. Thus the SDW fragments would have ferromagnetic components.

On the other hand, the result obtained by the neutron scattering measurements for PdCr is quite similar to that for PdMn; the satellite peak positions observed in both alloys are at $1 \pm \delta \ 0 \ 0$ reciprocal lattice points and are dependent on the solute concentration, but the satellite peak linewidth is not sensitive to the solute concentration. The SDW modulation vector $Q (= 1 - \delta)$ increases with increasing solute concentration. We do not repeat the discussion of a relation between the SDW wave vector Q and the actual shape of the Fermi surfaces in Pd metal. These results suggest that the mechanism of the spin-glass behavior for PdCr is the same as that for PdMn, therefore, the same as that for CuMn. Temperature variation of the satellite diffuse peak intensity given in Fig. 5 supports this point. The satellite peak intensity survives far above T_F determined by the susceptibility measurement. The data suggest that the most of the SDW clusters are still fluctuating above T_F with frequencies lower than the time resolution window of the neutron experiments ($\sim 10^{11}\text{Hz}$). For CuMn alloys, Werner and Gottaas¹² showed that the temperature at which the satellite peak disappears comes down close to the T_F when the time resolution window of neutron scattering is tightened. The similar feature would be expected for the PdCr SDW clusters.

In spite of the fact that the contents of PdCr alloys are different both in solute and in solvent from those of CuMn alloys, the same mechanism, the fluctuating SDW clusters, plays an essential role in the spin-glass-like behavior for

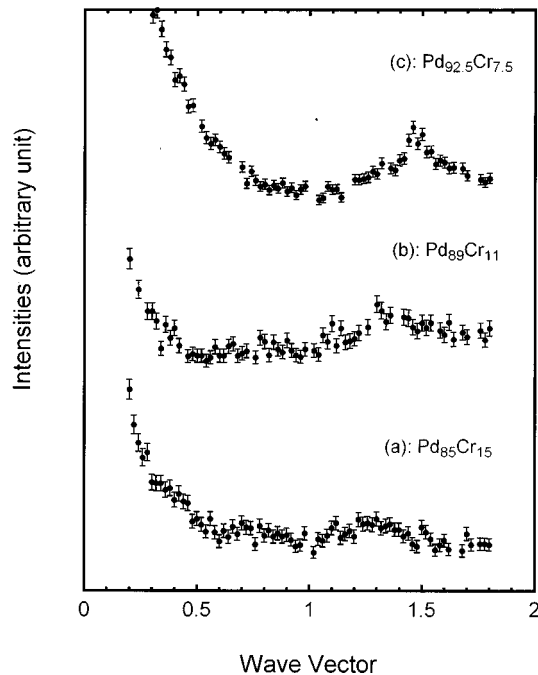


FIG. 6. Diffraction patterns for PdCr alloys [(a) 15 at. % Cr, (b) 11 at. % Cr, and (c) 7.5 at. % Cr] observed at far above the freezing temperature by scanning along the $[100]$ direction.

these systems. These data lead to an important conclusion that the fluctuating SDW clusters are the fundamental mechanism to stabilize the metallic spin-glass alloys, such as CuMn, AgMn,¹³ PdMn, PtMn,¹⁴ and PdCr.

Although the basic pictures of PdCr and PdMn alloys are very similar, there exist several differences between them. First the peak position δ is different; the δ value of PdCr is slightly larger than that of PdMn. In other word, modulation wavelength is longer for PdCr than for PdMn. On the other hand, the correlation length of PdCr is shorter than that of PdMn. This means that the cluster size in PdCr is smaller. The biggest difference is, however, that PdMn alloys have a Cu_3Au type atomic short-range order, which leads to a strong ASRO peak at 100. Since the neutron scattering amplitude of Mn is negative, the ASRO peak is distinctively observed even for a rather small SRO parameter. Although PdCr alloys have no atomic short-range order peak at 100 as shown in Fig. 3, very weak satellite diffuse peaks remain even at room temperature. These peaks are temperature independent. The special feature of these satellite reflection is asymmetry of the scattering intensities; on the contrary to the magnetic peaks, peak intensity at large Q position $(1 + \delta 0 0)$ is stronger than that at small Q position $(1 - \delta 0 0)$ as shown in Fig. 6. Similar temperature independent satellite reflections are observed more distinctively for nonmagnetic alloys such as PtV,¹⁵ PdV,¹⁵ and PtCr (Ref. 16) alloys and explained as the concentration wave of the constituent atoms accompanied with the lattice deformation wave. Details of the concentration wave will be published separately.¹⁷ In the present paper, we simply note that the concentration wave amplitude looks to be larger for the alloys with lower Cr concentration, for which the magnetic satellite peaks are far weaker. Roles of the concentration wave and the SDW, which come from

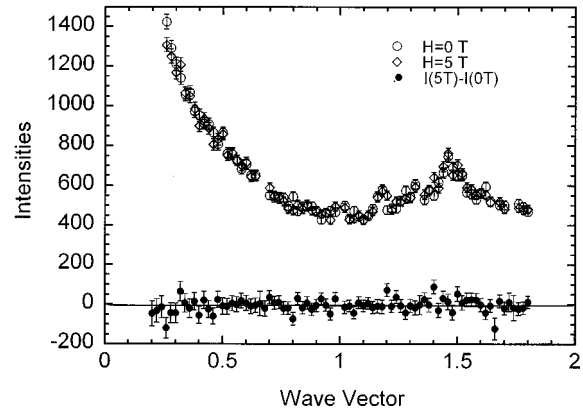


FIG. 7. Field dependence of the scattering intensity for $\text{Pd}_{92.6}\text{Cr}_{7.5}$.

the charge screening and magnetic screening of the impurities, respectively, are very interesting problems in connection with the Kondo singlet state.

Resistivity measurements for PdCr alloys show the minimum value at certain temperature for the alloys with Cr concentration lower than 7 at.%,⁹ suggesting that Cr has a localized moment. On the other hand, as we mentioned above, PdCr alloy containing less than the critical concentration is explained as a nonmagnetic state. The reason is that the Kondo singlet state is formed at low temperature due to rather high Kondo temperature ($T_K \approx 100$ K). Increasing of Cr concentration leads to recovery of the localized moment by the magnetic field of near neighbor solute spins and the spin-glass phase seems to be stabilized at low temperature. Then, it may be interesting problem to examine the recovery of the localized magnetic moment under the external magnetic field for PdCr alloys. If the localized magnetic moments recover under the magnetic field, these induced moments would couple together through the RKKY interaction and the induced satellite reflections could be observed like more concentrated alloys. Our specimen with 7.5 at. % Cr alloys seems to be located at the critical concentration. To study this point, such an experiment was performed for 7.5 at. % Cr alloy at 1.7 K under the magnetic field of 5 T and the data were compared with those without magnetic field. Experimental data are given in Fig. 7. There was no appreciable change of the satellite reflections in this experimental conditions as shown by the subtracted data $I(5\text{ T}) - I(0\text{ T})$. In place of the field induced satellite peaks, we observed temperature induced satellite reflections for decreasing temperature as shown in Fig. 4(c), indicating that Cr has a localized moment at this Cr concentration. The Kondo singlet state for PdCr alloys with lower Cr concentration is left for a future problem.

ACKNOWLEDGMENTS

The authors are indebted to Professor K. Kakurai and Dr. M. Nishi for helping us in the measurements at the 5 G (PONTA) spectrometer under the high magnetic field and low temperature.

- ¹J. W. Cable, S. A. Werner, G. P. Felcher, and N. Wakabayashi, Phys. Rev. B **29**, 1268 (1984).
- ²S. A. Werner, Comments Condens. Matter Phys. **15**, 55 (1990).
- ³Y. Tsunoda, N. Kumitomi, and J. W. Cable, J. Appl. Phys. **57**, 3753 (1985).
- ⁴T. M. Harders and P. Wells, J. Phys. F **13**, 1017 (1973).
- ⁵Y. Tsunoda, N. Hiruma, J. L. Robertson, and J. W. Cable, Phys. Rev. B **56**, 11 051 (1997).
- ⁶R. W. Cochrane, J. O. Ström-Olsen, and Gwyn Williams, J. Phys. F **9**, 1165 (1977).
- ⁷S. Chakravorty, P. Panigrahy, and Paul. A. Beck, J. Appl. Phys. **42**, 1697 (1971).
- ⁸J. A. Mydosh and G. J. Nieuwenhuys, *Ferromagnetic Materials I* (North-Holland, Amsterdam, 1980), p. 71.
- ⁹R. M. Roshko and Gwyn Williams, Phys. Rev. B **16**, 1503 (1977).
- ¹⁰F. C. C. Kao and Gwyn Williams, Phys. Rev. B **7**, 267 (1973).
- ¹¹S. C. Ho, I. Maartense, and Gwyn Williams, Phys. Rev. B **24**, 5174 (1971).
- ¹²S. A. Werner, J. J. Rhyne, and J. A. Gotaas, Solid State Commun. **56**, 457 (1983).
- ¹³K. Ishibashi, Y. Tsunoda, N. Kumitomi, and J. W. Cable, Solid State Commun. **56**, 585 (1985).
- ¹⁴T. Sunaga and Y. Tsunoda (unpublished).
- ¹⁵Y. Tsunoda, J. Magn. Magn. Mater. **177–181**, 1337 (1998).
- ¹⁶M. Hirano and Y. Tsunoda (unpublished).
- ¹⁷A. Murakami and Y. Tsunoda (unpublished).